Tetrahedron: *Asymmetry* xxx (2013) xxx–xxx

Contents lists available at SciVerse ScienceDirect

Tetrahedron: *Asymmetry*

journal homepage: www.elsevier.com/locate/tetasy

Chiral *para*-alkyl phenyl ethers of glycerol: synthesis and testing of chirality driven crystallization, liquid crystal, and gelating properties

Alexander A. Bredikhin *, Dmitry V. Zakharychev, Robert R. Fayzullin, Olga A. Antonovich, Alexander V. Pashagin, Zemfira A. Bredikhina

A.E. Arbuzov Institute of Organic and Physical Chemistry of Kazan Scientific Center of Russian Academy of Sciences, Arbuzov St., 8, Kazan 420088, Russian Federation

ARTICLE INFO

Article history:
Received 8 April 2013
Accepted 24 May 2013
Available online xxxx

ABSTRACT

A series of enantiopure and racemic *p*-alkylphenyl glycerol ethers **1a**–**k** were synthesized. A new, sensitive, and pictorial method of comparison of the IR spectra of solid enantiopure and racemic samples was developed to obtain preliminary information on the crystallization types of these compounds. In order to detect the subtle differences in the organization of the chiral solid phase, a new easily implemented approach, based on a chromatographic measuring of the relative abundance of the enantiomers in a single solution in equilibrium with a solid sample of arbitrary ($0 < ee < 1$) composition, is reported. One new conglomerate compound (Alk = *n*-Pr) and one borderline case (Alk = *n*-Bu) are disclosed. Higher members of the series of **1** (starting with an *n*-Bu derivative) are turned into liquid crystals upon melting; no significant differences between racemic and non-racemic samples were found. Only enantiopure methyl-, *n*-butyl, *n*-pentyl, *n*-hexyl, and *n*-heptyl substituted **1** were able to form supramolecular gels in hydrocarbon solvents; all racemic ethers **1** did not show such ability.

1. Introduction

The behavior of chiral molecules in the formation of ordered systems is stereoselective. Thus, during the process of nucleation and crystal growth of the racemic material, both enantiomers may be involved in a number of successive chiral discrimination acts; this leads to the formation of different types of crystalline racemate.[1] In most cases, a molecular racemic compound arises, that is, a heterochiral crystal lattice is formed from the identical, and balanced in terms of enantiomeric composition, unit cells. Racemic conglomerates consisting of enantiopure crystals are less common, but nonetheless are often formed. Together, these two cases cover more than 90% of the actual chiral crystals. In rare cases, the crystalline phase is either a solid solution or an exotic anomalous racemate.[1,2]

In all cases, information on the nature of the crystallization of the target products has tremendous value to organic-practitioners. If successful, one can take advantage of stereoselective crystallization to obtain the enantiopure product, in addition to establishing a multi-step strategy for its synthesis on a solid theoretical basis.[2]

So called 'soft matters', such as liquid crystals and gels formed by polymeric and low molecular weight gelators (LMWG), are the subject of constant interest in organic chemistry.[3] The relationship between the properties of such 'soft matter' and the enantiomeric composition of the parent substance is well-known for chiral compounds.[4,5] This relationship is due to differences in the nature of self-assembly of chiral molecules, and to an extent the nature of their crystallization.[6,7] Consequently, information about the type of chiral crystalline phase is essential during the search for new, and the modification of known 'soft matters'.

A noteworthy example of chiral discrimination involves the simplest chiral organogelator *p*-tolyloxypropane-1,2-diol **1a**. We have shown that a high gelling ability is inherent in (*R*)- and (*S*)-**1a**, while *rac*-**1a** does not form any supramolecular gels.[8] Herein we continued the search of LMWG among other *para*-substituted phenyl glycerol ethers, *rac*-, and *scal*-3-(4-alkylphenoxy)-propane-1,2-diols **1a**–**k** (Scheme 1).

Previously Tschierske et al. have reported that the members of the racemic diol family **1** exhibit properties of thermotropic liquid crystals (LC).[9] On the other hand, we have shown that diols *rac*-**1a** and *scal*-**1a** not only form metastable phases during the melt crystallization, but also show pronounced chiral discrimination in this process.[7] Investigation into the effect of the chirality on the manifestation of liquid crystal properties within the **1b**–**k** family is also another aim herein.

Variously substituted phenyl glycerol ethers have been investigated in our previous studies, and it was shown that these compounds are characterized by a high frequency of conglomerate formation.[2] An important goal herein is to demonstrate new techniques, which use standard conditions in a synthetic laboratory equipment, to obtain valuable information about the subject.

* Corresponding author. Tel.: +7 843 2319167; fax: +7 843 2731872.
E-mail address: baa@iopc.ru (A.A. Bredikhin).

0957-4166/$ - see front matter © 2013 Elsevier Ltd. All rights reserved.
http://dx.doi.org/10.1016/j.tetasy.2013.05.017

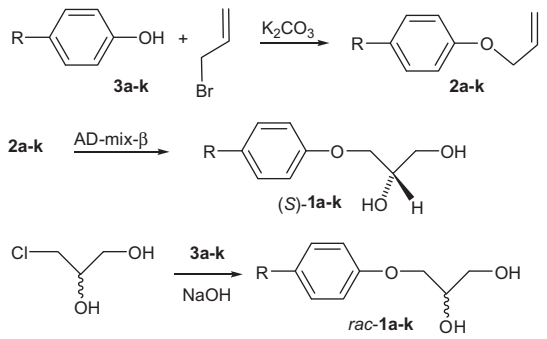

R = CH_3 **a**, C_2H_5 **b**, *i*-C_3H_7 **c**, *n*-C_3H_7 **d**, *tert*-C_4H_9 **e**, *n*-C_4H_9 **f**, *n*-C_5H_{11} **g**, *n*-C_6H_{13} **h**, *n*-C_7H_{15} **i**, *n*-C_8H_{17} **j**, *n*-C_9H_{19} **k**.

Scheme 1. Synthesis and designation of the studied compounds.

2. Results and discussion

2.1. Chemistry

Herein non-racemic samples of *scal*-3-(4-alkylphenoxy)-propane-1,2-diols **1a**–**k** were obtained from allyloxyalkyl benzenes **2a**–**k** through Sharpless asymmetric dihydroxylations (SAD).[10] Earlier Wang et al., using methyl, methoxy, chloro, and cyanosubstituted allyloxybenzenes as examples, demonstrated that dihydroxylation of *ortho*-substituted allyl ethers took place with low enantioselectivity (products ee 28–63%), whereas the results for *para*-substituted derivatives are satisfactory (ee 89–95%).[11] In the same paper, it was also found that the use of AD-mix-β as a reagent gave products with an (*S*)-configuration at the C2 carbon atom. Our results are consistent with these conclusions. Ethers **2a-k**, precursors of the target compounds, were obtained with moderate yields (~60–70%) from the corresponding phenols **3a**–**k** and allyl bromide under the action of a base (K_2CO_3). To obtain racemic diols *rac*-**1a**–**k**, we used the interaction of *rac*-3-chloropropane-1,2-diol with the corresponding phenolates. Our approach to the target compounds is outlined in Scheme 1. Some experimental characteristics of the diols investigated are shown in Table 1.

Listed in the third column of Table 1, the values of the enantiomeric excess for non-racemic diols **1a**–**k** refer to the primary reaction products, which were studied immediately after the SAD reaction had finished. As expected, the length and degree of branching of the alkyl substituent did not affect the enantioselectivity of the reaction. It is possible to increase the enantiomeric purity to ee ⩾99% by simple recrystallization (fourth column) for all of the diols except for *tert*-butyl derivative **1e**. In this case, it is impossible to increase the starting ee value by subsequent crystallizations; this could mean that the composition of the eutectics for this substance is characterized by ee_{eu} >91%.

Valuable information on the nature of the crystallization of a chiral substance can be obtained from a comparison of its racemic and enantiomerically enriched (scalemic) sample melting points, the value $\Delta T^f_{r,s} = T^f_r - T^f_s$, shown in Table 1. The positive $\Delta T^f_{r,s}$ values for **1a**–**c**, **e**, and **g**–**j** indicate the formation of racemic compounds by these substances in the solid phase. A value of $\Delta T^f_{r,s} \geqslant 30$°C points to high racemic compound stability in the case of **1e**. This information, in conjunction with the above data on the composition of the eutectics, is sufficient to conclude that the chiral substance **1e** could be attributed to a type of 'anticonglomerates'.

For compounds **1d**, **1f,** and **1k** the $\Delta T^f_{r,s}$ quantities are negative and significant in absolute values: −14, −16, and −43 °C in the order listed. Such melting points indicate that these compounds may exhibit the property of spontaneous resolution during crystallization. However other considerations should be taken into account for definitive conclusions; for example, one could compare the vibration spectra of these compounds in the solid phase.

2.2. IR spectroscopy

A comparison of the IR spectra of crystalline racemic and enantiomeric samples is often used to determine the type of chiral crystallization. In this case, the similarity of the IR spectra shows the similarity of the crystal structure of the samples and may indicate that the test substance crystallizes as a conglomerate. In contrast, the IR spectra of a racemic compound are usually different to those of their respective enantiomers.[1a,13] The main difficulty associated with this approach consists of establishing reliable criteria for the similarities and differences of complex spectroscopic curves.

Modern instruments record the spectra in digital form. Typically, such a spectrum represents a two-dimensional digital array (A_i, ν_i), where ν_i stands for the vibrational frequency (usually expressed in wave numbers in increments of 1 cm^{-1}), and A_i corresponds to the extinction at this wave number. If the ν value for the two arrays changes with the same step, the standard Pearson correlation coefficient **r** can be used for their quantitative comparison. This coefficient, calculated for two arrays $\{A^R_i\}$ and $\{A^A_i\}$ (superscripts R and A denote racemic and scalemic samples), was proposed by us as a quantitative complement to traditional visual comparison of normalized spectra.[14] Building on this approach, for a more detailed and demonstrable comparison of the vibrational

Table 1
Yield and enantiomeric excess of asymmetric dihydroxylation products (*S*)-**1a**–**k** and some physicochemical characteristics of *rac*- and *scal*-**1a**–**k**

Diol	Yield (%)	ee[a] (%)		Mp (°C)		$\Delta T^f_{r,s}$	cp[b] (°C)	
		Before	After	*rac* (lit.)	*scal*		*rac* (lit.)	*scal*
1a	48	88.8	99.0	74–75 (70)[c]	68	7–6	—	—
1b	43	91.5	99.5	68 (66)[c]	61–62	7–6	—	—
1c	53	92.5	99.0	58–60	57	3–1	—	—
1d	57	86.5	99.7	68 (49.5)[c]	82	-14	— (67.5) [c]	—
1e	72	91.0	<91	85–87 (84–86)[d]	55	32–30	—	—
1f	79	91.1	99.9	54 (53)[c]	70	-16	75 (75)[c]	75
1g	59	90.0	99.6	65 (57)[c]	52	13	80 (80.5)[c]	78
1h	61	89.8	99.1	63 (60)[c]	48	15	85 (87)[c]	85
1i	65	91.4	99.7	66 (61)[c]	51.5	14.5	86 (88)[c]	85
1j	70	90.8	99.7	65 (58)[c]	60	5	89 (91)[c]	89
1k	68	90.7	99.2	69 (55.5)[c]	112	−43	90 (92.5)[c]	—

[a] Enantiomeric excess of diols (*S*)-**1a**–**k** before and after recrystallization.
[b] Clearing point.
[c] Ref. 9.
[d] Ref. 12.

spectra herein, we decided to use a graphical representation of the correlation between the two spectra, that is, visually display them in the coordinates A_i^R versus A_i^A. Figure 1 illustrates the features of this approach.

The right hand side of Figure 1 shows the parts of the conditional spectra, several peaks of which are simulated by a Gaussian with $\sigma = 5$ cm^{-1}. One of the spectroscopic curves (called a model spectrum) is shown as a set of different colored segments; the second (reference spectrum) is shown as a thin black line. Each pair of peaks illustrates the most common real situation accompanied the spectra comparison, such as the coincidence of the bands, the difference in frequency or intensity, and baseline drift. Left of the figure shows the trajectories arising from the correlation of a pair of spectral lines in the coordinates of the transmittance intensity A_i^R versus A_i^A. The color of the trajectory linking two correlated spectrum, which is a graphical representation of a particular situation, matches the color of the model spectrum fragment. It can be seen that the proposed procedure is very sensitive to the context and can reliably detect even slight differences of spectra lines in frequency and/or intensity. Secondly, the shape of the correlation trajectory is informative and makes it easy to identify a particular type of mismatch. Of course, the real spectra can differ by several parameters simultaneously. However, the proposed procedure retains its attractiveness in this case as well.

It is clear that the proposed procedure is applicable not only to compare the spectra of chiral compounds, but also to identify subtle and non-obvious differences between any of the digital spectra. For pairwise comparison of the experimental arrays we wrote a simple program 'Trajectory' that uses the open source mathematical package Sage. It allows a user to display the original spectra, the correlation trajectories, as well as to select and analyze fragments of the spectra in interactive mode.

The experimental IR spectra recorded for the crystal samples **1a**–**k** (pellets in KBr), and the correlation coefficients and correlation trajectories for each pair of 'racemate-scalemate' are shown in Figure 2. It can be seen that the new criterion can easily ascertain the essential difference in the spectra of the racemate and scalemate for substances **1a**–**c**, **e**, and **g**–**k**, without going into a detailed analysis of the spectroscopic differences. Thus, despite the fact that the correlation coefficient between pairs of spectra for **1c**, **1e**, **1h**, and **1j** amounted to 0.95 or more, in all these cases the appearance of the trajectory leaves no doubt with regard to the essential differences between the crystal structures of racemic and homochiral samples. For compound **1k**, the correlation coefficient ($r = 0.948$) as well as the 'spreading' of the correlation trajectory over the area cannot be attributed to racemic conglomerates. The reason for the abnormally high difference between the melting point of the racemate and scalemate for this compound, found in Section 2.1, will be explained in Section 2.4.

Two compounds, *n*-propyl and *n*-butyl-substituted diols **1d** and **1f** fall out of the total number under the comparison of the IR spectra. The high value of $r = 0.998$ and the compact nature of the correlation trajectory allow us to assign with a considerable degree of certainty the diol **1d** to the family of conglomerate formative compounds. The correlation coefficient for the diol **1f** was also high ($r = 0.994$). However, analysis of the correlation trajectory reveals non-obvious differences in the spectra of *rac*- and *scal*-**1f** by visual inspection (Fig. 3).

As can be seen from Figure 3, we can see at least three spectroscopic components at 535, 1055, and 2955 cm^{-1}, for which there are small spectroscopic shifts in the transition from the racemic solid phase to the enantiopure. The differences in the spectra are minimal, but the pattern of the changes is difficult to attribute to the influence of impurities in the material or matrix. These results led us to doubt that in this case we were dealing with a conglomerate. At the same time, the similarity of the spectra in the region of hydrogen bonds O–H···O led us to conclude that the experimental spectra belong to the crystal structure, which has an almost identical system of intra- and intermolecular hydrogen bonds.

In order to accurately determine the type of crystallization of racemic compounds **1d** and **1f**, we have developed another simple technique that enables fast and reliable determination of the eutectic composition of the chiral matter on the basis of experimental data on the solubility of the sample of an intermediate enantiomeric composition. In addition to the diols **1d**, **f**, we also investigated diol **1b**, which, as we now know, forms a racemic compound in the solid phase.

2.3. Solubility test

One indication of the crystallization of a chiral compound as a conglomerate is the 'Meyerhoffer's double solubility rule',[15] which follows from simple thermodynamic considerations. Let us consider a ternary heterogeneous system 'stereoisomers + achiral solvent', in which the dissolution is not accompanied by dissociation or association of stereoisomers, in terms of the thermodynamic activity of its components. As the 'origin' for such a system, it naturally accepts a crystalline phase of a pure enantiomer, the activity

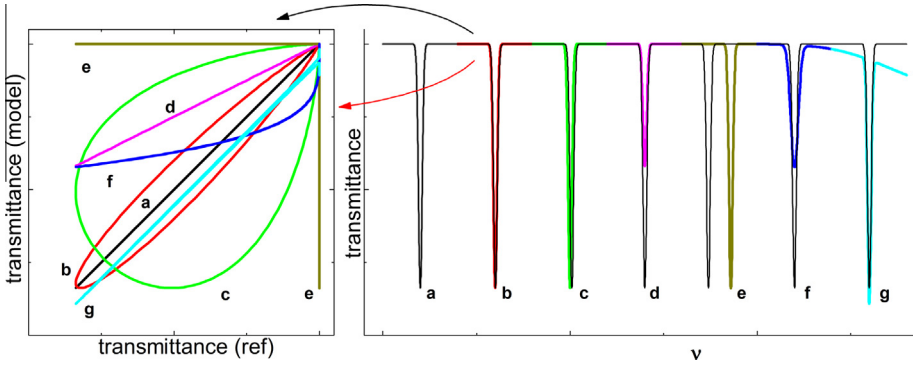

Figure 1. Two conditional spectra A_i^R and A_i^A and their correlation in the axes A_i^R versus A_i^A. The reference spectrum (right panel) is shown as a black line, the bands in the model spectrum and the corresponding bands' correlation images (left panel) are shown as the colored fragments. Illustrated are the following cases: (a, black) peaks are identical, the correlation trajectory lies on the diagonal tg $\alpha = 1$; (b, red) intensities are identical, a small (1 cm^{-1}) shift in frequency, the trajectory is a narrow loop around the diagonal; (c, green) significant (5 cm^{-1}) shift in frequency, wide loop; (d, magenta) peaks vary in height (2 times), straight line, deviating from the diagonal the stronger, the more differences; (e, dark yellow) peaks are completely separated (or the corresponding peak is absent in one of the spectra), the trajectory degenerates into a horizontal and/or vertical lines; (f, blue) peaks have an identical integral extinction but differ two times in extinction at the maximum, the trajectory is curved; (g, cyan) peaks are observed on the background of a baseline shift of one of the spectra, a trajectory that is parallel to the diagonal.

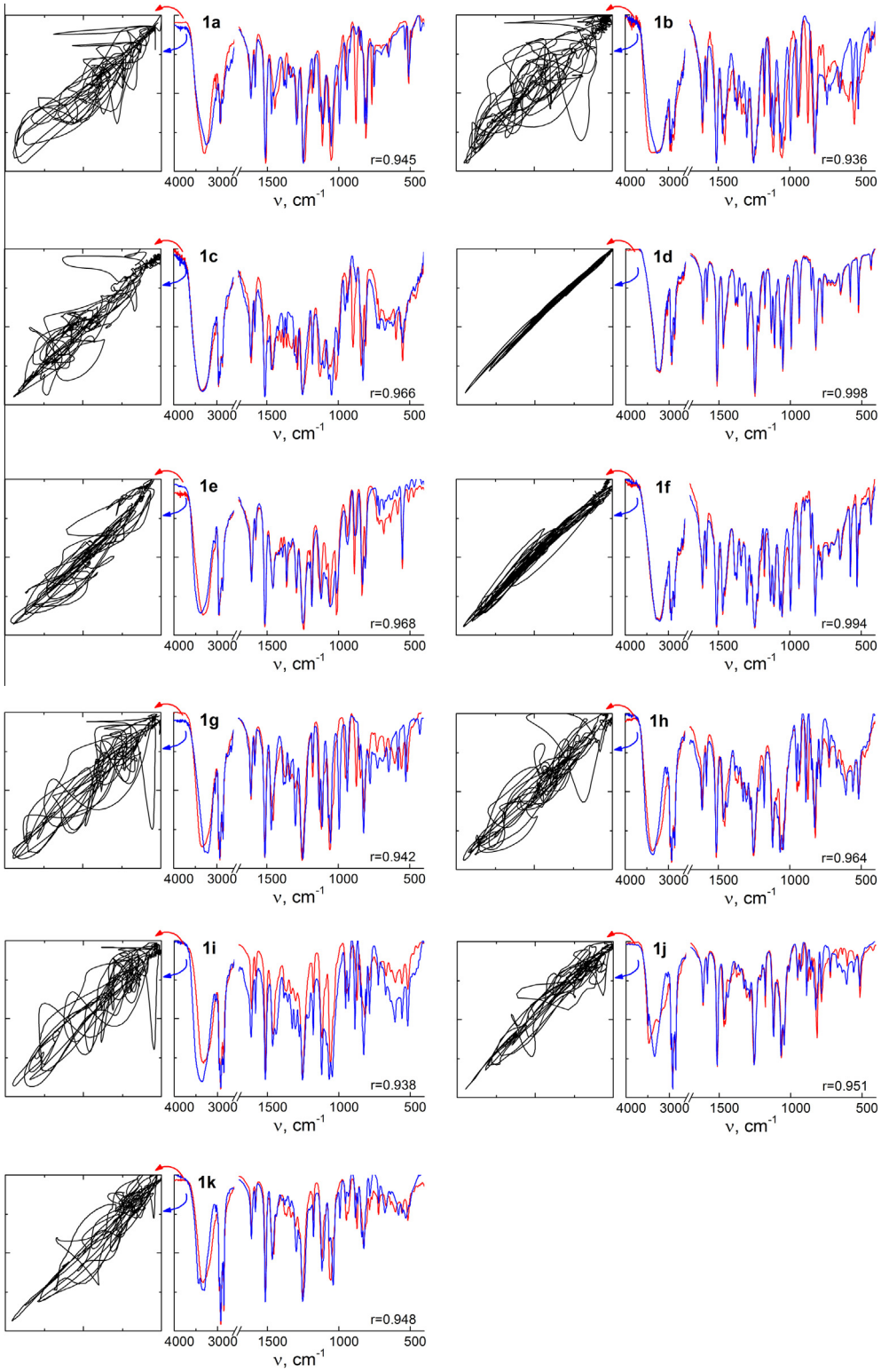

Figure 2. IR spectra of racemic and enantiopure samples **1a–k** and graphical representation of the correlations between them.

of which is by definition equal to unity. In an equilibrium state between the solid phase and solution (i.e., for a saturated solution) the activity of the components in the solution and in the solid phase is equal. Thus, the activity of an individual stereoisomer in its saturated solution is also equal to unity. For a conglomerate (assuming no mutual solubility of enantiomers in solid state) solid phase is represented by a mechanical mixture of enantiopure crystals of two enantiomers. Therefore, in this case the activities of each of the enantiomers in a saturated solution are equal to unity. However, since the solvent is achiral, activity coefficients of enantiomers are the same, the concentrations of both enantiomers are also equal. If the solubility of the enantiomers is not too large, we can neglect the dependence of the activity coefficient on the concentration and believe that each of these concentrations is

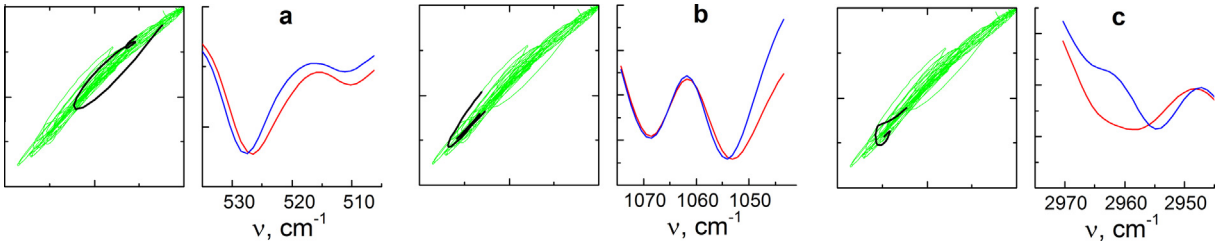

Figure 3. Typical loop-type fragments of the correlation trajectory (black lines) and the corresponding regions of the experimental IR spectra of racemic (red curves) and enantiopure (blue curves) crystalline samples of diol **1f** in the KBr matrix.

equal to the concentration of a saturated solution of the individual stereoisomers. Accordingly, the total concentration of a substance in a saturated solution of a conglomerate should be twice as high as in the saturated solution of an enantiopure substance.

For a racemic compound, the activities of the enantiomers in the solid phase are not equal to unity. If formed, the racemic compound must be thermodynamically preferred over the conglomerate, and therefore begin to crystallize from solution prior to the (potential) racemic conglomerate, provided that at the beginning of the crystallization, the concentration of each of the enantiomers would be lower than for a saturated solution of the conglomerate. This means that the activity of the enantiomers for a saturated solution of the racemic compound, and therefore for its crystal phase, should be less than unity, and the ratio of its solubility to the solubility of the individual enantiomers is less than two.

It is clear that the activity of an enantiopure substance, which forms an individual phase in the solid sample, is unity even though the (excess) enantiomer is mixed with the phase of the racemic compound. Its activity in a solution in equilibrium with this mixture should also be equal to unity. Consequently, the equilibrium concentration of the excess isomer [to be specific, let it be (*R*)-isomer] corresponds to its solubility in enantiopure form:

$$[R]_{eu} = C^{A}_{sat} \tag{1}$$

while the composition of the solution corresponds to the composition of the eutectics and is unambiguously determined by the solubility ratio of its components through the solubility product (P_{sol}):

$$P_{sol} = [R]_{eu} \cdot [S]_{eu} = const \tag{2}$$

The expressions (1) and (2) were obtained on an empirical basis and tested on experimental data in the work of Klussmann et al.[16]

Generally speaking, the composition of the eutectics for a chiral substance explicitly identifies the type of its crystallization. Based on this we propose a simple and effective test. For its use we require a solid sample containing simultaneously both enantiomers in unequal amounts (i.e., integral enantiomeric purity of this sample $1 > ee > 0$). In practice, such a sample is easy to prepare by mixing approximately equal amounts of the racemate and enantioenriched substance. The amount of the solid sample and solvent are selected so that both enantiomers must be left in the solid in equilibrium with a saturated solution. The relative equilibrium concentration of the enantiomers in this saturated solution can be easily determined by chiral chromatography. The composition of the eutectics could be calculated on the basis of these data by the formula:

$$x_{eu}(\text{mole fraction, m.f.}) = \frac{[R]_{eu}}{[R]_{eu} + [S]_{eu}} \tag{3}$$

The results of the chromatographic analysis of saturated solutions in equilibrium with the two-component solid phases for compounds **1b**, **d**, and **f** are shown in lines 1–2 of Table 2. The eutectic compositions of these compounds, calculated by formula (3), are shown in line 3. The statistical characteristics (including confidence intervals computed using standard statistical procedures) show the high accuracy of this parameter, and consequently, the high resolution of the proposed test. Our experience has shown that the eutectic composition can be accurately determined in one measurement, and that the procedure does not require us to determine the absolute values of concentration and thus conduct preliminary calibrations.

Table 2
The results of chromatographic determination of the concentration of individual enantiomers $[R]_{eu}$ and $[S]_{eu}$ in solutions in equilibrium with a mixture of the crystals of the racemate and scalemate, and the eutectic compositions x_{eu} of the corresponding systems, which are found on this basis, as well as the concentration of saturated cyclohexane solutions of enantiopure $\left(C^{A}_{sat}\right)$ and racemic $\left(C^{Rc}_{sat}\right)$ samples of diols **1b**, **d**, and **f**

Line	Parameter	Compound		
		1b	**1d**	**1f**
1	$[S]_{eu}$	0.12 (0.01)	0.98 (0.04)	0.92 (0.03)
2	$[R]_{eu}$	0.96 (0.04)	0.98 (0.04)	1.01 (0.03)
3	x_{eu} (m.f.)[a]	0.888 (0.001)	0.501 (0.001)	0.521 (0.005)
4	C^{Rc}_{sat} [b]	0.68 (0.02)	1.97 (0.07)	1.93 (0.06)
5	C^{Rc}_{sat}	0.69 (0.03)	1.94 (0.07)	1.91 (0.06)
6	C^{A}_{sat}	1.00 (0.05)	1.00 (0.12)	1.00 (0.05)
7	x_{eu} (m.f.)[c]	0.90 (0.01)	0.51 (0.02)	0.53 (0.03)

The concentrations are presented as areas of the corresponding chromatographic peak, normalized to the average peak area of a saturated solution of the enantiopure substances. Statistical confidence intervals ($\alpha = 0.95$) of the corresponding values are indicated in parentheses.
[a] Calculated by the formula (3).
[b] Calculated by the formula (4).
[c] Calculated by the formula (5).

Table 2 shows that for **1d**, a value of $x_{eu} = 0.5$ was determined with an accuracy of ~0.2%, which allows us to attribute this diol to the family of conglomerate formatting compounds. At the same time, the composition of the eutectics for **1f** ($x_{eu} = 0.521$) is statistically significantly different from the value of 0.5, indicating the formation of a racemic compound by this system. Even more telling is the same test for compound **1b** ($x_{eu} = 0.89$), for which the formation of a racemic compound follows immediately from other above cited data.

It should also be noted that the same results of a single measurement of the relative composition of the equilibrium solution in prescribed conditions, along with eutectic composition, provide additional information about the system. According to equation (1), the peak area of the predominant stereoisomer (Table 2, line 2) corresponds to the solubility of enantiopure substance. The product of the same areas of the peaks corresponds to the solubility product, the scope of which extends to the racemic composition. Combining equations (1) and (2), the solubility of the racemate can be easily calculated from the equation:

$$C^{Rc}_{sat} = 2 \cdot \sqrt{[R]_{eu} \cdot [S]_{eu}} \tag{4}$$

The calculated values using this formula are shown in line 4 of Table 2. For the sake of comparison, the chromatographic data directly obtained for the solutions of enantiopure and racemic samples in equilibrium with the corresponding solid phases are shown in lines 5 and 6.

It is natural that the data for the equilibrium solutions of racemic and enantiopure samples (Table 2, lines 5–6) can also be used for the eutectic composition estimate according to the formula:

$$x_{eu}(\text{m.f.}) = \frac{1}{1 + \left(\frac{C^{Rc}_{sat}}{2 \cdot C^{A}_{sat}}\right)^2} \quad (5)$$

The results of the calculation (line 7) were in good agreement with the values determined by formula (3) (line 3), although the latter were much more accurate.

Thus, our proposed approach, with minimal experimental effort, provides a way of reliable identification of the main types of crystallization of chiral substances and simultaneously allows us to receive almost the same amount of information on the solubility of racemic and enantiopure phase as does the direct determination of these quantities. At the same time, this procedure does not require a sample with high enantiomeric purity, and also allows measurements at room temperature without special temperature control.

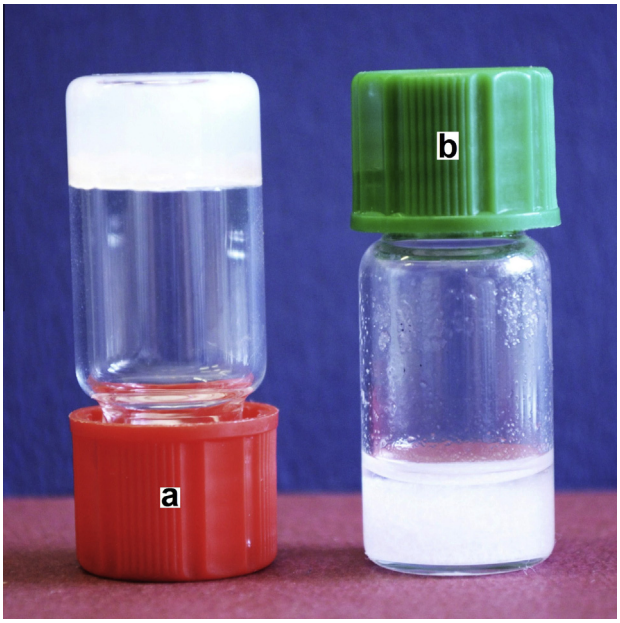

Figure 4. Gel formed by (*S*)-**1g** in hexane (a) and crystals of *rac*-**1g**, obtained under the same conditions (**b**).

2.4. Liquid crystalline properties

We next studied the behavior of diols **1a**–**k** upon heating. Compounds **1a**–**e** when heated at melting point immediately formed a clear isotropic liquid phase. The melting of the high-order members of the series, compounds **1f**–**k**, went through two steps: after the complete disappearance of the solid phase, a turbid anisotropic liquid phase was formed, which upon further heating became transparent. Such a behavior is typical of compounds forming a thermotropic liquid crystalline phase, which with a temperature increase becomes an isotropic liquid.

In addition to the melting point (mp), the temperatures of this last transition (clearing point, cp) are also given in Table 1. The melting and clearing points for compounds *rac*-**1d**, **f**–**k** were defined by Tschierske et al.[9] In general, our findings are consistent with the literature, with some differences noted in Table 1. As can be seen from Table 1, no significant differences between the values of cp for the racemic and enantiomeric samples of the same compound were observed. At first glance, the nonyl substituted diol seems to be an exception. In this case the sample of *scal*-**1k** melts to form an isotropic phase, so that its clearing point is missing. However in this case, the hypothetical transition temperature of the metastable LC phase to isotropic liquid (by analogy with other members of the series $cp_{scal} \sim cp_{rac} \sim 90$ °C) is reached before the melting of the crystals ($mp_{scal} = 112$ °C). Apparently, it is this factor, which explains the large value $\Delta T^{f}_{r,s}$, which was discussed in Sections 2.1 and 2.2. If for all the other diols the investigated thermoinitiated phase transition, designated as the 'melting point', describes homogeneous processes (notably transition 'crystal-isotropic liquid' for **1a**–**e**, or 'crystal-LC mesophase' for **1f**–**j**), then for the last member the transition temperature 'crystal-LC mesophase' for *rac*-**1k** is compared with a transition temperature 'crystal-isotropic liquid' for *scal*-**1k**. Thermodynamics imposes no obvious limitations on the relationship of such temperatures.

2.5. Gelation abilities

Recently, we found that the *para*-tolyl glycerol ether **1a** is the simplest known chiral organogelator with pronounced chirality driven properties. While the non-racemic samples of *scal*-**1a** of both configurations indicate a high tendency to supramolecular gelation, *rac*-**1a** is completely devoid of gelation properties.[8] The *ortho*- and *meta*-tolyl glycerol ethers revealed no low molecular weight gelator (LMWG) abilities either in racemic or enantiopure form.[7] In order to identify general regularities that govern gelation in the series of aromatic ethers of glycerol, we examined this ability for *para*-alkylsubstituted diols **1b**–**k**. We found that the non-racemic diols *scal*-**1f**–**i** exhibited an ability to gel formation in a hydrocarbon medium (here after the results for *n*-hexane are given), to form stable opaque supramolecular gels, in which the fraction of gelator amounts to 0.8–1.6 wt %. A typical gel formed by (*S*)-**1g** (1 wt % in hexane) is shown in Figure 4a. At the same time, none of the investigated racemic diols showed an ability to form a supramolecular gel in organic solvents. Under the same conditions, most of the racemic derivatives formed thin plate-like crystals (similar to that shown for the racemate in Fig. 4b). It should be noted that non-racemic diols *scal*-**1b**–**d**, **j**–**k** also crystallized within the same concentration range, but formed the needle crystals of an elongated shape.

The relationship between the gelation and crystallization peculiarities for LMWG of similar structures was studied earlier.[17] Usually this fact is associated with different crystallization types of the corresponding samples. This was the case for all of the investigated racemic and enantiopure diols **1**, with the exception of compounds **1d**, **f**. However, based on the nature of the crystals, the non-racemic diols form close to each other resulting in crystal packing. Another reason for the different gelation ability of compounds with a similar structure is their solubility.[18] Apparently, this is the reason for the different results obtained for non-racemic diols **1**. Both factors, the crystal structure and the solubility, will be investigated in subsequent studies.

3. Conclusion

A series of enantiomeric and racemic *p*-alkylphenyl terminal glycerol ethers, 3-(*p*-alkylphenoxy)-propane-1,2-diols **1a**–**k** were synthesized by the SAD method from allyl phenyl ethers and the reaction of the corresponding phenols with racemic 3-chloropropane-1,2-diol. In order to obtain preliminary information on the

types of chirality that drove the crystallization, a new pictorial method of the comparison of the IR spectra of solid enantiopure and racemic samples was developed. This method consists of the construction and analysis of the correlation trajectories between the pairs of spectra. Testing this approach for the entire set of diols synthesized allowed the identification of eight new cases of the formation of racemic compounds, and allowed us to detect a new case of spontaneous resolution (*n*-propyl derivative **1d**) and a borderline case of *n*-butyl derivative **1f**.

In order to detect the subtle differences in the organization of the solid phase of a chiral substance another new method was offered, based on measuring the relative abundance of the enantiomers in the solution in equilibrium with a solid sample of arbitrary intermediate ($0 < ee < 1$) composition. Using only the chromatogram of this solution (if the separation of the peaks of enantiomers is achieved) allowed us to accurately determine the composition of the eutectic and as a result, reliably characterize the type of crystallization of the substance. A value of $x_{eu} = 0.5$ indicated crystallization of the product in the form of a conglomerate, whereas an x_{eu} value different from 0.5 indicated the formation of a racemic compound.

Higher members of the series of diols **1** (starting with *n*-butyl derivative **1f**) were turned into liquid crystals upon melting. No significant differences in the behavior of racemic and non-racemic samples were found in these cases. On the contrary, the ability of *para*-alkylphenyloxypropanediols to form supramolecular gels in hydrocarbon solvents inherits the expressed chirality driven character. The properties of the low molecular weight organogelator are common to enantiopure samples of methyl-, *n*-butyl, *n*-pentyl, *n*-hexyl, and n-heptylsubstituted diols **1a**, **f**–**i**. All of the studied compounds in racemic, and diols **1b**–**e**, **j**–**k** in enantiopure form do not show such ability. Apparently, for racemic samples the reason for this lies with the qualitative features of the crystal packing, and for enantiomeric samples—with the solubility (which is in turn related to the energy of the crystal lattice).

4. Experimental

4.1. General

The NMR spectra were recorded on a Bruker Avance-400 (399.9 MHz for ^{1}H; 100.5 MHz for ^{13}C) spectrometer in $CDCl_3$ with TMS or the signals of the solvent as the internal standard (the signals of the aromatic protons in ^{1}H NMR spectra for all diols **1a**–**k** and aryl allyl ethers **2a**–**k** are present as a typical AA′BB′ system). The IR spectra of the polycrystalline samples of *rac*- and (*S*)-diols **1a**–**k** in KBr pellets were recorded on a Bruker Tensor 27 spectrometer. Optical rotations were measured on a Perkin–Elmer model 341 polarimeter (concentration *c* is given as g/100 mL). Mass-spectra EI were recorded on a mass-spectrometer DFS Thermo Electron Corporation (70 eV). Melting points and clearing points (cp) of liquid crystal-isotropic melt transmissions for general purposes were determined using a Boëtius apparatus and are uncorrected. HPLC analyses were performed on a Shimadzu LC-20AD system controller and UV monitor 275 nm was used as a detector. The columns used, from Daicel, Inc., were Chiralcel OD-H (0.46 × 25 cm), Chiralpak AD (0.46 × 25 cm), Chiralcel OJ (0.46 × 25 cm).

4.2. Synthesis

Racemic 3-chloropropane-1,2-diol (99+%) was purchased from Acros Organics; 4-ethylphenol (97%), 4-isopropylphenol (98%), 4-*n*-butylphenol (98%), 4-*n*-pentylphenol (98%), 4-*n*-heptylphenol (98 + %), 4-*n*-octylphenol (99%), 4-*n*-nonylphenol (98+%), and allyl bromide (99%) were purchased from Alfa Aesar; 4-propylphenol (99%), 4-hexylphenol (⩾98%), AD-mix-alpha, and AD-mix-beta were from Aldrich.

4.2.1. General procedure for the synthesis of aryl allyl ethers 2a–k

Aryl allyl ethers were prepared according to the published method.[19] A stirred suspension of the appropriate phenol **3a**–**k** (6 mmol), allyl bromide (0.8 g, 6.6 mmol), and ground water-free K_2CO_3 (0.91 g, 6.6 mmol) in anhydrous acetone (10 mL) was refluxed for approximately 12–14 h; the progress of the reaction was monitored by TLC analysis (for product $R_f \sim 0.7$; eluent: hexane/EtOAc = 9:1). The reaction mixture was diluted with water (30 mL) and extracted with Et_2O (3 × 40 mL). The collected organic phases were washed with 1 M NaOH (15 mL) and dried over $MgSO_4$. The solvent was removed under reduced pressure to afford ether **2a**–**k** as fluid oil. The crude product was purified by column chromatography (silica gel, eluent: hexane/EtOAc = 9:1–8:2).

4.2.1.1. 1-(Allyloxy)-4-methylbenzene 2a. Yield: 64%, bp 82–83 °C (8 Torr), $n_D^{23} = 1.5162$; [lit.[20] bp 100–100.5 °C (9 Torr), $n_D^{25} = 1.5157$]. ^{1}H NMR δ 2.30 (s, 3H, CH_3), 4.53 (ddd, J = 1.5, 5.3 Hz; 2H, OCH_2), 5.29 (ddt, J = 1.5, 1.5, 10.5 Hz; 1H, CH_2), 5.42 (ddt, J = 1.5, 1.5, 17.3 Hz; 1H, CH_2), 6.07 (ddt, J = 5.3, 10.5, 17.3 Hz; 1H, CH), 6.82–6.85 (m, 2H, Ar), 7.07–7.11 (m, 2H, Ar). EI mass-spectrum [m/z (I)]: 148(79), 133(32), 107(73), 91(19), 77(92), 65(16), 51(24), 41(100).

4.2.1.2. 1-(Allyloxy)-4-ethylbenzene 2b. Yield: 68%, bp 91 °C (8 Torr), $n_D^{23} = 1.5164$; [lit.[20] bp 96–96.8 °C (9 Torr), $n_D^{25} = 1.5124$]. ^{1}H NMR δ 1.19 (t, J = 7.5 Hz; 3H, CH_3), 2.57 (q, J = 7.5 Hz, 2H, CH_2), 4.48 (ddd, J = 1.5, 5.1 Hz; 2H, OCH_2), 5.24 (ddt, J = 1.5, 1.5, 10.6 Hz; 1H, CH_2), 5.42 (ddt, J = 1.5, 1.5, 17.3 Hz; 1H, CH_2), 6.07 (ddt, J = 5.3, J = 10.5, 17.3 Hz; 1H, CH), 6.80–6.84 (m, 2H, Ar), 7.06–7.10 (m, 2H, Ar). EI mass-spectrum [m/z (I)]: 162(53), 147(44), 133(27), 121(31), 107(33), 93(48), 91(60), 65(19), 51(16), 41(100).

4.2.1.3. 1-(Allyloxy)-4-isopropylbenzene 2c. Yield: 70%, bp 105–106 °C (8 Torr), $n_D^{23} = 1.5053$; [lit.[21] bp 93–94 °C (6 Torr); lit.[22] $n_D^{25} = 1.5074$]. ^{1}H NMR δ 1.25 (d, J = 6.9 Hz; 6H, CH_3), 2.89 (septet, J = 6.9 Hz; 1H, CH), 4.56 (ddd, J = 1.5, 5.3 Hz; 2H, OCH_2), 5.31 (ddt, J = 1.5, 1.5, 10.5 Hz; 1H, CH_2), 5.43 (ddt, J = 1.5, 1.5, 17.2 Hz; 1H, CH_2), 6.07 (ddt, J = 5.3, 10.5, 17.2 Hz; 1H, CH), 6.86–6.90 (m, 2H, Ar), 7.13–7.17 (m, 2H, Ar). EI mass-spectrum [m/z (I)]: 176(35), 161(100), 133(13), 121(16), 105(21), 91(65), 77(20), 55(9), 41(79).

4.2.1.4. 1-(Allyloxy)-4-propylbenzene 2d. Yield: 67%, bp 116 °C (8 Torr), $n_D^{23} = 1.5052$. ^{1}H NMR δ 0.96 (t, J = 7.4 Hz; 3H, CH_3), 2.57 (sextet, J = 7.4 Hz; 2H, CH_2), 2.55 (t, J = 7.4 Hz; 2H, CH_2), 4.54 (ddd, J = 1.5, 5.3 Hz; 2H OCH_2), 5.30 (ddt, J = 1.5, 1.5, 10.5 Hz; 1H, CH_2), 5.44 (ddt, J 1.5, 1.5, 17.3 Hz; 1H, CH_2), 6.07 (ddt, J = 5.3, 10.5, 17.3 Hz; 1H, CH), 6.85–6.88 (m, 2H, Ar), 7.09–7.28 (m, 2H, Ar). EI mass-spectrum [m/z (I)]: 176(31), 147(88), 119(11), 107(45), 93(21), 91(28), 65(24), 51(10), 41(100).

4.2.1.5. 1-(Allyloxy)-4-*tert*-butylbenzene 2e. Yield: 55%, bp 114 °C (8 Torr), $n_D^{23} = 1.5050$; [lit.[21] bp 115–116 °C (8 Torr); lit.[23] $n_D^{24} = 1.5058$]. ^{1}H NMR δ 1.33 (s, 9H, CH_3), 4.55 (ddd, J = 1.6, 5.3 Hz; 2H, OCH_2), 5.29 (ddt, J = 1.6, 1.6, 10.5 Hz; 1H, CH_2), 5.43 (ddt, J = 1.6, 1.6, 17.3 Hz; 1H, CH_2), 6.07 (ddt, J = 5.3, 10.5, 17.3 Hz; 1H, CH), 6.86–6.90 (m, 2H, Ar), 7.30–7.35 (m, 2H, Ar). EI mass-spectrum [m/z (I)]: 190(17), 175(100), 147(6), 135(11), 105(23), 91(28), 77(15), 65(10), 55(9), 41(59).

4.2.1.6. 1-(Allyloxy)-4-*n*-butylbenzene 2f. Yield: 63%, bp 126–127 °C (8 Torr), $n_D^{23} = 1.5063$. ^{1}H NMR δ 0.94 (t, J = 7.3 Hz; 3H,

CH_3), 1.33–1.39 (m, 2H, CH_2CH_3), 1.55–1.60 (m, 2H, $CH_2CH_2CH_2$), 2.56 (t, J = 7.7 Hz; 2H, CH_2), 4.53 (ddd, J = 1.5, 5.3 Hz; 2H, OCH_2), 5.28 (ddt, J = 1.5, 1.5, 10.5 Hz; 1H, CH_2), 5.42 (ddt, J = 1.5, 1.5, 17.3 Hz; 1H, CH_2), 6.07 (ddt, J = 5.3, 10.5, 17.3 Hz; 1H, CH), 6.84–6.86 (m, 2H, Ar), 7.09–7.11 (м, 2H, Ar). EI mass-spectrum [m/z (I)]: 190(31), 147(100), 133(8), 107(43), 91(25), 77(18), 65(17), 41(99).

4.2.1.7. 1-(Allyloxy)-4-*n*-pentylbenzene 2g. Yield: 67%, bp 135 °C (8 Torr), $n_D^{23} = 1.5047$. ^{1}H NMR δ 0.91 (t, J = 7.3 Hz; 3H, CH_3), 1.31–1.39 (m, 4H, $CH_2(CH_2)_2CH_3$), 1.55–1.63 (m, 2H, $CH_2CH_2CH_2$), 2.56 (t, J = 7.7 Hz; 2H, CH_2), 4.53 (ddd, J = 1.5, 5.3 Hz; 2H, OCH_2), 5.28 (ddt, J = 1.5, 1.5, 10.5 Hz; 1H, CH_2), 5.42 (ddt, J = 1.5, 1.5, 17.3 Hz; 1H, CH_2), 6.07 (ddt, J = 5.3, 10.5, 17.3 Hz; 1H, CH), 6.84–6.86 (m, 2H, Ar), 7.05–7.13 (m, 2H, Ar). EI mass-spectrum [m/z (I)]: 204(21), 147(100), 119(9), 107(34), 91(17), 77(11), 65(10), 41(99).

4.2.1.8. 1-(Allyloxy)-4-*n*-hexylbenzene 2h. Yield: 68%, $n_D^{23} = 1.5030$. ^{1}H NMR δ 0.94 (t, J = 6.8 Hz, 3H, CH_3), 1.31–1.40 (m, 6H, $CH_2(CH_2)_3CH_3$), 1.59–1.67 (m, 2H, $CH_2CH_2CH_2$), 2.59 (t, J = 7.7 Hz; 2H, CH_2), 4.56 (ddd, J = 1.5, 5.3 Hz; 2H, OCH_2), 5.32 (ddt, J = 1.5, 1.5, 10.5 Hz; 1H, CH_2), 5.45 (ddt, J = 1.5, 1.5, 17.3 Hz; 1H, CH_2), 6.11 (ddt, J = 5.3, 10.5, 17.3 Hz; 1H, CH), 6.86–6.90 (m, 2H, Ar), 7.11–7.15 (m, 2H, Ar). EI mass-spectrum [m/z (I)]: 218(18), 147(100), 133(8), 107(34), 91(18), 77(12), 55(8), 41(79).

4.2.1.9. 1-(Allyloxy)-4-*n*-heptylbenzene 2i. Yield: 69%, $n_D^{23} = 1.4958$. ^{1}H NMR δ 0.90 (t, J = 7.3 Hz; 3H, CH_3), 1.31–1.48 (m, 8H, $CH_2(CH_2)_4CH_3$), 1.55–1.63 (m, 2H, $CH_2CH_2CH_2$), 2.55 (t, J = 7.7 Hz; 2H, CH_2), 4.53 (ddd, J = 1.5, 5.3 Hz; 2H, OCH_2), 5.28 (ddt, J = 1.5, 1.5, 10.5 Hz; 1H, CH_2), 5.42 (ddt, J = 1.5, 1.5, 17.3 Hz; 1H, CH_2), 6.07 (ddt, J = 5.3, 10.5, 17.3 Hz; 1H, CH), 6.84–6.86 (m, 2H, Ar), 7.05–7.12 (m, 2H, Ar). EI mass-spectrum [m/z (I)]: 232(26), 147(100), 107(32), 91(15), 77(8), 55(10), 41(74).

4.2.1.10. 1-(Allyloxy)-4-*n*-octylbenzene 2j. Yield: 67%, $n_D^{23} = 1.4989$. ^{1}H NMR δ 0.91 (t, J = 6.9 Hz; 3H, CH_3), 1.30–1.40 (m, 10H, $CH_2(CH_2)_5CH_3$), 1.55–1.63 (m, 2H, $CH_2CH_2CH_2$), 2.56 (t, J = 7.8 Hz; 2H, CH_2), 4.54 (ddd, J = 1.5, 5.3 Hz; 2H, OCH_2), 5.30 (ddt, J = 1.5, 1.5, 10.5 Hz; 1H, CH_2), 5.43 (ddt, J = 1.5, 1.5, 17.3 Hz; 1H, CH_2), 6.09 (ddt, J = 5.3, 10.5, 17.3 Hz; 1H, CH), 6.84–6.87 (m, 2H, Ar), 7.08–7.12 (m, 2H, Ar). EI mass-spectrum [m/z (I)]: 246(24), 147(100), 133(9), 107(29), 91(11), 77(7), 55(7), 41(65).

4.2.1.11. 1-(Allyloxy)-4-*n*-nonylbenzene 2k. Yield: 61%, $n_D^{23} = 1.4964$. ^{1}H NMR δ 0.90 (t, J = 6.8 Hz; 3H, CH_3), 1.30–1.38 (m, 12H, $CH_2(CH_2)_6CH_3$), 1.54–1.61 (m, 2H, $CH_2CH_2CH_2$), 2.55 (t, J = 7.7 Hz; 2H, CH_2), 4.53 (ddd, J = 1.5, 5.3 Hz; 2H, OCH_2), 5.28 (ddt, J = 1.5, 1.5, 10.5 Hz; 1H, CH_2), 5.42 (ddt, J = 1.5, 1.5, 17.3 Hz; 1H, CH_2), 6.07 (ddt, J = 5.3, 10.5, 17.3 Hz; 1H, CH), 6.84–6.86 (m, 2H, Ar), 7.05–7.12 (m, 2H, Ar). EI mass-spectrum [m/z (I)]: 260(15), 147(100), 133(8), 107(29), 91(12), 77(6), 55(7), 41(65).

4.2.2. General procedure for the synthesis of racemic 3-(4-alkylphenoxy)-propane-1,2-diols 1a–k

Racemic diols **1a**–**k** were synthesized in a manner similar to the literature.[24] To a stirred solution of phenol **3a**–**k** (15 mmol) in EtOH (9 mL) a solution of NaOH (0.72 g, 18 mmol) in water (3 mL) was added. The resulting mixture was stirred and heated at reflux for 2 h. After cooling to 50 °C, *rac*-3-chloropropane-1,2-diol (1.95 g, 17.6 mmol) in 3 mL of EtOH was added slowly and the reaction mixture was stirred and heated at reflux for a further 10–15 h; the termination time of the reaction was determined by TLC analysis. After cooling, the reaction mixture was diluted with water (70 mL) and extracted with Et_2O (3 × 60 mL). The collected organic layers were washed with 1 M NaOH (15 mL) and dried over $MgSO_4$. The solvent was removed under reduced pressure to obtain a solid residue or oil, which was crystallized in hexane at −10 °C. The crude diols were purified by recrystallization from hexane/EtOAc = 5:1 to give pure products as a white crystalline material with 65–71% yield. The melting and cleaning points for diols *rac*-**1a**–**k** are given in Table 1. NMR spectra were identical with those cited below for corresponding (*S*)-**1a**–**k**.

4.2.3. General procedure for the asymmetric dihydroxylation process

Sharpless asymmetric dihydroxylation process (SAD) was carried out according to the literature.[11] A stirred solution of AD-mix (1.4 g) in *t*-BuOH (5 mL) and water (5 mL) was cooled to 0 °C. To the suspension, aryl allyl ether **2a**–**k** (1 mmol) was added and then the reaction mixture was stirred intensively at 0 °C for 20 h. Next, Na_2SO_3 (1.5 g) was added and stirred at room temperature for 30 min. The *t*-BuOH layer was separated and the aqueous layer was extracted with EtOAc (3 × 30 mL). The combined organic layers were washed with brine (20 mL), dried over $MgSO_4$, and concentrated under reduced pressure to give the product as crystals or as an oil. If needed, the crude product was purified by column chromatography (silica gel, eluent: hexane/EtOAc = 8:2–4:6). Yields and enantiomeric excesses of the prepared diols *scal*-**1a**–**k** are shown in Table 1. The use of AD-mix-β gave (*S*)-enantiomers. For analytical purposes, the diols were purified by recrystallization from hexane/EtOAc = 5:1 to give pure products as white crystalline materials.

4.2.3.1. (*S*)-3-(4-Methylphenoxy)-propane-1,2-diol (*S*)-1a. Mp 68 °C, $[\alpha]_D^{20} = +9.1$ (*c* 0.8, EtOH), 99.0% ee [chiral HPLC analysis; Daicel Chiralpak AD column; column temperature 22 °C; eluent: 2-propanol/hexane = 1:4; flow rate: 1 mL/min; t_R = 7.4 min (minor), t_R = 8.4 min (major)]; [lit.[8] mp 67–69 °C, $[\alpha]_D^{20} = +9.0$ (*c* 0.8, EtOH), 96% ee; lit.[25] for (*R*)-**1a**: $[\alpha]_D^{20} = -9.2$ (*c* 1.0, EtOH), 97% ee]. ^{1}H NMR δ 2.14 (t, J = 5.9 Hz, 1H, OH), 2.28 (s, 3H, CH_3), 2.70 (d, J = 4.3 Hz, 1H, OH), 3.72–3.77 (m, 1H, CH_2OH), 3.81–3.86 (m, 1H, CH_2OH), 3.99–4.05 (m, 2H, CH_2O), 4.06–4.09 (m, 1H, $CHOH$), 6.81 (m, 2H, Ar), 7.08 (m, 2H, Ar). ^{13}C NMR δ 20.4, 63.7, 69.4, 70.4, 114.5, 130.0, 130.6, 153.3.

4.2.3.2. (*S*)-3-(4-Ethylphenoxy)-propane-1,2-diol (*S*)-1b. Mp 61–62 °C, $[\alpha]_D^{20} = +6.7$ (*c* 1.2, EtOH), 99.5% ee [chiral HPLC analysis; Daicel Chiralcel OD-H column; column temperature 27 °C; eluent: 2-propanol/hexane = 3:17; flow rate: 1.0 mL/min; t_R = 9.0 min (minor), t_R = 11.2 min (major)]. ^{1}H NMR δ 1.22 (t, J = 7.6 Hz; 3H, CH_3), 2.29 (br s, 2H, OH), 2.61 (q, J = 7.6 Hz; 2H, CH_2), 3.76 (dd, J = 5.4, 11.4 Hz; 1H, CH_2OH), 3.85 (dd, J = 3.8, 11.4 Hz; 1H, CH_2OH), 4.01–4.07 (m, 2H, CH_2O), 4.09–4.14 (m, 1H, $CHOH$), 6.83–6.90 (m, 2H, Ar), 7.10–7.17 (m, 2H, Ar). ^{13}C NMR δ 15.8, 28.0, 63.7, 69.4, 70.44, 114.5, 128.8, 137.2, 156.5. Anal. Calcd for $C_{11}H_{16}O_3$: C, 67.32; H, 8.22. Found: C, 67.24; H, 8.28.

4.2.3.3. (*S*)-3-(4-Isopropylphenoxy)-propane-1,2-diol (*S*)-1c. Mp 57 °C, $[\alpha]_D^{20} = +6.7$ (*c* 1.0, EtOH), 99.0% ee [chiral HPLC analysis; Daicel Chiralcel OD-H column; column temperature 22 °C; eluent: 2-propanol/hexane = 1:9; flow rate: 1.0 mL/min; t_R = 16.7 min (minor), t_R = 21.3 min (major)]. ^{1}H NMR δ 1.24 (d, J = 7.0 Hz; 6H, CH_3), 2.32 (br s, 2H, OH), 2.88 (septet, J = 7.0 Hz; 1H, CH), 3.76 (dd, J = 5.4, 11.4 Hz; 1H, CH_2OH), 3.85 (dd, J = 3.8, 11.4 Hz; 1H, CH_2OH), 4.01–4.07 (m, 2H, CH_2O), 4.09–4.14 (m, 1H, $CHOH$), 6.84–6.89 (m, 2H, Ar), 7.13–7.19 (m, 2H, Ar). ^{13}C NMR δ 24.2, 33.3, 63.7, 69.2, 70.4, 114.4, 127.4, 141.7, 156.5. Anal. Calcd for $C_{12}H_{18}O_3$: C, 68.54; H, 8.63. Found: C, 68.43; H, 8.55.

4.2.3.4. (*S*)-3-(4-*n*-Propylphenoxy)-propane-1,2-diol (*S*)-1d. Mp 82 °C, $[\alpha]_D^{20} = +7.2$ (*c* 1.0, EtOH), $[\alpha]_D^{20} = +7.3$ (*c* 0.98, MeOH), 99.7% ee [chiral HPLC analysis; Daicel Chiralcel OD-H column; column

temperature 27 °C; eluent: 2-propanol/hexane = 1:9; flow rate: 1.0 mL/min; t_R = 15.9 min (minor), t_R = 21.2 min (major)]. ^{1}H NMR δ 0.94 (t, J = 7.5 Hz; 3H, CH_3), 1.62 (sextet, J = 7.5 Hz; 2H, CH_2), 1.99 (br s, 2H, OH), 2.54 (t, J = 7.5 Hz; 2H, CH_2), 3.76 (dd, J = 5.4, 11.4 Hz; 1H, CH_2OH), 3.85 (dd, J = 3.8, 11.4 Hz; 1H, CH_2OH), 4.01–4.07 (m, 2H, CH_2O), 4.08–4.15 (m, 1H, C*H*OH), 6.81–6.87 (m, 2H, Ar), 7.07–7.13 (m, 2H, Ar). ^{13}C NMR δ 13.7, 24.7, 37.1, 63.7, 69.3, 70.4, 114.4, 129.44, 135.64, 156.5. Anal. Calcd for $C_{12}H_{18}O_3$: C, 68.54; H, 8.63. Found: C, 68.68; H, 8.45.

4.2.3.5. (*S*)-3-(4-*tert*-Butylphenoxy)-propane-1,2-diol (*S*)-1e. The crude product (*S*)-**1e** was purified by column chromatography. Mp 55 °C, $[\alpha]_D^{20} = +6.6$ (*c* 1.0, EtOH), $[\alpha]_D^{20} = +6.2$ (*c* 0.6, MeOH), 91.0% ee. [For reliable *ee* determination the crude diol was transformed into a diastereomeric mixture of cyclic sulfites via reaction between *scal*-**1e** (1 equiv) and $SOCl_2$ (1.5 equiv) in CH_2Cl_2 at 0 °C. Chiral HPLC analysis of the reaction mixture: Daicel Chiralcel OJ column; column temperature 22 °C; eluent 2-propanol/hexane = 3:7, flow rate 1.0 mL/min; t_R = 10.9 min (major), t_R = 17.4 min (major), t_R = 27.7 min (minor), t_R = 46.5 min (minor).] {Lit.[25] $[\alpha]_D^{20} = +7.5$ (*c* 1.0, EtOH), >99% ee}. ^{1}H NMR δ 1.32 (s, 9H, CH_3), 2.18 (br s, 2H, OH), 3.76 (dd, J = 5.3, 11.4 Hz; 1H, CH_2OH), 3.85 (dd, J = 3.7, 11.4 Hz; 1H, CH_2OH), 4.02–4.08 (m, 2H, CH_2O), 4.09–4.14 (m, 1H, C*H*OH), 6.85–6.89 (m, 2H, Ar), 7.30–7.34 (m, 2H, Ar). ^{13}C NMR δ 31.5, 34.1, 63.7, 69.3, 70.4, 114.1, 126.34, 144.1, 156.1. Anal. Calcd for $C_{13}H_{20}O_3$: C, 69.61; H, 8.99. Found: C, 69.43; H, 9.03.

4.2.3.6. (*S*)-3-(4-*n*-Butylphenoxy)-propane-1,2-diol (*S*)-1f. Mp 70 °C, cp 75 °C, $[\alpha]_D^{20} = +6.6$ (*c* 1.0, EtOH), 99.9% ee [chiral HPLC analysis; Daicel Chiralcel OD-H column; column temperature 27 °C; eluent: 2-propanol/hexane = 1:9; flow rate: 1.0 mL/min; t_R = 15.9 min (minor), t_R = 19.3 min (major)]. ^{1}H NMR δ 0.93 (t, J = 7.3 Hz; 3H, CH_3), 1.35 (sextet, J = 7.3 Hz, 2H, CH_2CH$_3$), 1.53–1.62 (m, 2H, CH_2CH_2CH$_2$), 2.07 (br s, 2H, OH), 2.57 (t, J = 7.6 Hz; 2H, CH_2), 3.76 (dd, J = 5.4, 11.4 Hz; 1H, CH_2OH), 3.85 (dd, J = 3.8, 11.4 Hz; 1H, CH_2OH), 4.01–4.08 (m, 2H, CH_2O), 4.08–4.14 (m, 1H, C*H*OH), 6.83–6.86 (m, 2H, Ar), 7.09–7.13 (m, 2H, Ar). ^{13}C NMR δ 13.9, 22.3, 33.8, 34.7, 63.7, 69.4, 70.4, 114.2, 129.4, 135.8, 156.4. Anal. Calcd for $C_{13}H_{20}O_3$: C, 69.61; H, 8.99. Found: C, 69.45; H, 8.96.

4.2.3.7. (*S*)-3-(4-*n*-Pentylphenoxy)-propane-1,2-diol (*S*)-1g. Mp 52 °C, cp 78 °C, $[\alpha]_D^{20} = +7.6$ (*c* 1.0, EtOH), 99.6% ee [chiral HPLC analysis; Daicel Chiralcel OD-H column; column temperature 20 °C; eluent: 2-propanol/hexane = 1:9; flow rate: 1.0 mL/min; t_R = 13.2 min (minor), t_R = 18.9 min (major)]. ^{1}H NMR δ 0.91 (t, J = 6.9 Hz; 3H, CH_3), 1.27–1.39 (m, 4H, CH_2(CH_2)$_2$CH$_3$), 1.55–1.63 (quintet, J = 7.5 Hz; 2H, CH_2CH_2CH$_2$), 2.22 (br s, 2H, OH), 2.56 (t, J = 7.6 Hz; 2H, CH_2), 3.76 (dd, J = 5.4, 11.4 Hz; 1H, CH_2OH), 3.85 (dd, J = 3.8, 11.4 Hz; 1H, CH_2OH), 4.01–4.08 (m, 2H, CH_2O), 4.08–4.14 (m, 1H, C*H*OH), 6.83–6.87 (m, 2H, Ar), 7.09–7.13 (m, 2H, Ar). ^{13}C NMR δ 14.0, 22.5, 31.3, 31.4, 35.0, 63.7, 69.4, 70.4, 114.2, 129.4, 135.9, 156.4. Anal. Calcd for $C_{14}H_{22}O_3$: C, 70.56; H, 9.30. Found: C, 70.44; H, 9.21.

4.2.3.8. (*S*)-3-(4-*n*-Hexylphenoxy)-propane-1,2-diol (*S*)-1h. Mp 48 °C, cp 85 °C $[\alpha]_D^{20} = +6.4$ (*c* 1.0, EtOH), 99.1% ee [chiral HPLC analysis; Daicel Chiralcel OD-H column; column temperature 20 °C; eluent: 2-propanol/hexane = 1:9; flow rate: 1.0 mL/min; t_R = 12.2 min (minor), t_R = 17.5 min (major)]. ^{1}H NMR δ 0.91 (t, J = 6.8 Hz; 3H, CH_3), 1.28–1.40 (m, 6H, CH_2(CH_2)$_3$CH$_3$), 1.60 (quintet, J = 7.5 Hz; 2H, CH_2CH_2CH$_2$), 2.52 (s, 2H, OH), 2.57 (t, J = 7.6 Hz; 2H, CH_2), 3.77 (dd, J = 5.5, 11.4 Hz; 1H, CH_2OH), 3.85 (dd, J = 3.7, 11.4 Hz; 1H, CH_2OH), 4.01–4.08 (m, 2H, CH_2O), 4.09–4.15 (m, 1H, C*H*OH), 6.83–6.88 (m, 2H, Ar), 7.09–7.14 (m, 2H, Ar). ^{13}C NMR δ 14.5, 23.0, 29.4, 32.1, 32.2, 35.5, 64.2, 69.8, 70.9, 114.8, 129.8, 136.3, 156.9. Anal. Calcd for $C_{15}H_{24}O_3$: C, 71.39; H, 9.59. Found: C, 71.42; H, 9.68.

4.2.3.9. (*S*)-3-(4-*n*-Heptylphenoxy)-propane-1,2-diol (*S*)-1i. Mp 51.5 °C, cp 85 °C, $[\alpha]_D^{20} = +6.5$ (*c* 1.0, EtOH), 99.7% ee [chiral HPLC analysis; Daicel Chiralcel OD-H column; column temperature 20 °C; eluent: 2-propanol/hexane = 1:4; flow rate: 1.0 mL/min; t_R = 7.6 min (minor), t_R = 9.5 min (major)]. ^{1}H NMR δ 0.90 (t, J = 6.9 Hz; 3H, CH_3), 1.23–1.35 (m, 8H, CH_2(CH_2)$_4$CH$_3$), 1.59 (quintet, J = 7.5 Hz; 2H, CH_2CH_2CH$_2$), 1.85 (br s, 2H, OH), 2.56 (t, J = 7.6 Hz; 2H, CH_2), 3.77 (dd, J = 5.4, 11.4 Hz; 1H, CH_2OH), 3.86 (dd, J = 3.9, 11.4 Hz; 1H, CH_2OH), 4.01–4.08 (m, 2H, CH_2O), 4.09–4.15 (m, 1H, C*H*OH), 6.83–6.87 (m, 2H, Ar), 7.09–7.14 (m, 2H, Ar). ^{13}C NMR δ 14.1, 22.6, 29.1, 29.2, 31.7, 31.8, 35.0, 63.7, 69.4, 70.7, 114.2, 129.3, 135.9, 156.4. Anal. Calcd for $C_{16}H_{26}O_3$: C, 72.14; H, 9.84. Found: C, 72.38; H, 9.90.

4.2.3.10. (*S*)-3-(4-*n*-Octylphenoxy)-propane-1,2-diol (*S*)-1j. Mp 60 °C, cp 89 °C, $[\alpha]_D^{20} = +5.8$ (*c* 1.0, EtOH), ee 99.7% [chiral HPLC analysis; Daicel Chiralcel OD-H column; column temperature 20 °C; eluent: 2-propanol/hexane = 1:9; flow rate: 1.0 mL/min; t_R = 10.9 min (minor), t_R = 14.8 min (major)]. ^{1}H NMR δ 0.91 (t, J = 6.7 Hz; 3H, CH_3), 1.24–1.38 (m, 10H, CH_2(CH_2)$_5$CH$_3$), 1.60 (quintet, J = 7.5 Hz; 2H, CH_2CH_2CH$_2$), 1.95 (br s, 2H, OH), 2.57 (t, J = 7.6 Hz; 2H, CH_2), 3.77 (dd, J = 5.4, 11.4 Hz; 1H, CH_2OH), 3.86 (dd, J = 3.8, 11.4 Hz; 1H, CH_2OH), 4.02–4.09 (m, 2H, CH_2O), 4.09–4.16 (m, 1H, C*H*OH), 6.83–6.88 (m, 2H, Ar), 7.09–7.15 (m, 2H, Ar). ^{13}C NMR δ 14.5, 23.0, 29.7, 29.9, 32.1, 32.3, 35.5, 64.2, 69.8, 70.8, 114.8, 129.8, 136.3, 156.9. Anal. Calcd for $C_{17}H_{28}O_3$: C, 72.82; H, 10.06. Found: C, 72.71; H, 10.11.

4.2.3.11. (*S*)-3-(4-*n*-Nonylphenoxy)-propane-1,2-diol (*S*)-1k. Mp 112 °C, $[\alpha]_D^{20} = +5.3$ (*c* 0.5, MeOH), 99.2% ee [chiral HPLC analysis; Daicel Chiralcel OD-H column; column temperature 22 °C; eluent: 2-propanol/hexane = 1:4; flow rate: 1.0 mL/min; t_R = 5.8 min (minor), t_R = 6.9 min (major)]. ^{1}H NMR δ 0.90 (t, J = 6.9 Hz; 3H, CH_3), 1.22–1.36 (m, 12H, CH_2(CH_2)$_6$CH$_3$), 1.59 (quintet, J = 7.5 Hz; 2H, CH_2CH_2CH$_2$), 2.03 (br s, 2H, OH), 2.56 (t, J = 7.6 Hz; 2H, CH_2), 3.77 (dd, J = 5.4, 11.4 Hz; 1H, CH_2OH), 3.85 (dd, J = 3.9, 11.4 Hz; 1H, CH_2OH), 4.01–4.08 (m, 2H, CH_2O), 4.09–4.14 (m, 1H, C*H*OH), 6.82–6.88 (m, 2H, Ar), 7.08–7.14 (m, 2H, Ar). ^{13}C NMR δ 14.1, 22.6, 29.2, 29.3, 29.5, 29.6, 31.7, 31.9, 35.0, 63.7, 69.4, 70.4, 114.4, 129.3, 135.9, 156.4. Anal. Calcd for $C_{18}H_{30}O_3$: C, 73.43; H, 10.27. Found: C, 73.24; H, 10.38.

4.3. Determination of the solubility

The solubility of compounds **1c**, **d**, and **f** was determined by chromatographic measurements of the concentration of the saturated solution of these compounds in analytical grade cyclohexane. Racemic and enantiopure samples (approximately 10 mg), as well as their mixture in a 1:1 ratio were placed in glass vials (5 mL) fitted with a stirrer bar after which the solvent (4 mL) was added. The vessel was sealed with a ground-glass stopper; the contents were continuously stirred overnight at 20 ± 1 °C. The vessel was allowed to stand for 2–3 h without stirring for sedimentation of excessive solid phase, and then the liquid phase was sampled with a syringe. The solution was forced over a Teflon filter (Millex®-LH) with a pore diameter of 0.45 μm from one syringe to another. The conditions of the chromatographic measurements were identical to those described in Sections 4.1 and 4.2. The areas of the chromatographic peaks were used directly as a numerical characteristic of the equilibrium content of each of the stereoisomers in the liquid phase. For each system, there were at least two independent experiments; the chromatographic determination of the concentration within each run was repeated 2–3 times. The results for each sys-

tem were combined and subjected to standard statistical analysis to assess the confidence interval of the parameters ($n = 5–6$, $\alpha = 0.95$).

4.4. Gelation test

The corresponding diol **1a–k** (~0.035 mmol) and hexane (~1 mL) were placed in a 2 mL vial and heated until the solid was dissolved. The resulting solution was cooled in air to room temperature, and then left for 30 min at this temperature. The state of the materials was evaluated by the 'stable-to-inversion of a vial' method. The stable visually turbid gels were observed only for *scal*-diols **1f–i**.

References

1. (a) Jacques, J.; Collet, A.; Wilen, S. H. *Enantiomers, Racemates, and Resolutions*; Krieger Publishing Company: Malabar, Florida, 1994; (b) Coquerel, G. *Enantiomer* **2000**, *5*, 481–498.
2. Bredikhin, A. A.; Bredikhina, Z. A.; Zakharychev, D. V. *Mendeleev Commun.* **2012**, *22*, 171–180.
3. (a) Hamley, I. W. *Introduction to Soft Matter: Synthetic and Biological Self-Assembling Materials*; John Wiley & Sons: Chichester, 2007; (b) Murtola, T.; Bunker, A.; Vattulainen, I.; Deserno, M.; Karttunen, M. *Phys. Chem. Chem. Phys.* **2009**, *11*, 1869–1892; (c) Praprotnik, M.; Site, L. D.; Kremer, K. *Annu. Rev. Phys. Chem.* **2008**, *59*, 545–571; (d) Backov, R. *Soft Matter* **2006**, *2*, 452–464.
4. For reviews on chirality in liquid crystals see: (a) Tschierske, C. Nanoscale Stereochemistry in Liquid Crystals. In *Chirality at the Nanoscale: Nanoparticles, Surfaces, Materials and More*; Amabilino, D. B., Ed.; Wiley-VCH: Weinheim, 2009; pp 271–304 [chapter 9]; (b) Reddy, R. A.; Tschierske, C. *J. Mater. Chem.* **2006**, *16*, 907–961; (c) Goodby, J. W. *J. Mater. Chem.* **1991**, *1*, 307–318.
5. For reviews on chirality in gels, see: (a) Malik, S.; Fujita, N.; Shinkai, S. Gels as a Media for Functional Chiral Nanofibers. In *Chirality at the Nanoscale: Nanoparticles, Surfaces, Materials and More*; Amabilino, D. B., Ed.; Wiley-VCH: Weinheim, 2009; pp 93–114 [chapter 4]; (b) Smith, D. K. *Chem. Soc. Rev.* **2009**, *38*, 684–694; (c) Brizard, A.; Oda, R.; Huc, I. *Top. Curr. Chem.* **2005**, *256*, 167–218.
6. Hanabusa, K.; Yamada, M.; Kimura, M.; Shirai, H. *Angew. Chem., Int. Ed.* **1996**, *35*, 1949–1951.
7. Bredikhin, A. A.; Zakharychev, D. V.; Bredikhina, Z. A.; Gubaidullin, A. T.; Fayzullin, R. R. *CrystEngComm* **2012**, *14*, 211–222.
8. Bredikhin, A. A.; Bredikhina, Z. A.; Akhatova, F. S.; Gubaidullin, A. T. *Chem. Commun.* **2010**, *46*, 3523–3525.
9. Tschierske, C.; Hentrich, F.; Joachimi, D.; Agert, O.; Zaschke, H. *Liq. Cryst.* **1991**, *9*, 571–582.
10. Kolb, H. C.; VanNieuwenhze, M. S.; Sharpless, K. B. *Chem. Rev.* **1994**, *94*, 2483–2547.
11. Wang, Z.-M.; Zhang, X.-L.; Sharpless, K. B. *Tetrahedron Lett.* **1993**, *34*, 2267–2270.
12. Bredikhina, Z. A.; Savel'ev, D. V.; Bredikhin, A. A. *Russ. J. Org. Chem.* **2002**, *38*, 213–219.
13. Eliel, E. L.; Wilen, S. H.; Doyle, M. P. *Basic Organic Stereochemistry*; Wiley-Interscience: New York, 2001.
14. Bredikhin, A. A.; Bredikhina, Z. A.; Akhatova, F. S.; Zakharychev, D. V.; Polyakova, E. V. *Tetrahedron: Asymmetry* **2009**, *20*, 2130–2136.
15. Meyerhoffer, W. *Ber. Dtsch. Chem. Ges.* **1904**, *37*, 2604–2610.
16. Klussmann, M.; White, A. J. P.; Armstrong, A.; Blackmond, D. G. *Angew. Chem., Int. Ed.* **2006**, *45*, 7985–7989.
17. Adams, D. J.; Morris, K.; Chen, L.; Serpell, L. C.; Bacsa, J.; Day, G. M. *Soft Matter* **2010**, *6*, 4144–4156.
18. Hirst, A. R.; Coates, I. A.; Boucheteau, T. R.; Miravet, J. F.; Escuder, B.; Castelletto, V.; Hamley, I. W.; Smith, D. K. *J. Am. Chem. Soc.* **2008**, *130*, 9113–9121.
19. Claisen, L.; Eisleb, O. *Justus Liebigs Ann. Chem.* **1913**, *401*, 21–119.
20. Goering, H. L.; Jacobson, R. R. *J. Am. Chem. Soc.* **1958**, *80*, 3277–3285.
21. Taskinen, E. *J. Chem. Soc., Perkin Trans. 2* **2001**, 1824–1834.
22. le Noble, W. J.; Hayakawa, T.; Sen, A. K.; Tatsukami, Y. *J. Org. Chem.* **1971**, *36*, 193–196.
23. Stäubli, B.; Fretz, H.; Piantini, U.; Woggon, W.-D. *Helv. Chim. Acta* **1987**, *70*, 1173–1193.
24. Egri, G.; Kolbert, A.; Bálint, J.; Fogassy, E.; Novák, L.; Poppe, L. *Tetrahedron: Asymmetry* **1998**, *9*, 271–283.
25. Theil, F.; Weidner, J.; Ballschuh, S.; Kunath, A.; Schick, H. *J. Org. Chem.* **1994**, *59*, 388–393.